Possibility of superconductivity in graphite intercalated with alkaline earths investigated with density functional theory

Matteo Calandra and Francesco Mauri
Institut de Minéralogie et de Physique des Milieux Condensés, Case 115, 4 Place Jussieu, 75252, Paris Cedex 05, France
(Received 23 May 2006; published 18 September 2006)

Using density functional theory we investigate the occurrence of superconductivity in AC_6 with $A=\mathrm{Mg,Ca,Sr,Ba}$. We predict that at zero pressure, Ba and Sr should be superconducting with critical temperatures (T_c) 0.2 and 3.0 K, respectively. We study the pressure dependence of T_c assuming the same symmetry for the crystal structures at zero and finite pressures. We find that the SrC_6 and BaC_6 critical temperatures should be substantially enhanced by pressure. On the contrary, for CaC_6 we find that in the 0–5 GPa region, T_c weakly increases with pressure. The increase is much smaller than that shown in several recent experiments. Thus we suggest that in CaC_6 a continous phase transformation, such as an increase in staging, occurs at finite pressure. Finally we argue that, although MgC_6 is unstable, the synthesis of intercalated systems of the kind $Mg_xCa_{1-x}C_y$ could lead to higher critical temperatures.

DOI: 10.1103/PhysRevB.74.094507 PACS number(s): 63.20.Kr, 63.20.Dj, 78.30.Er

I. INTRODUCTION

It has long been known that graphite intercalated compounds (GICs) can display a superconducting behavior at low temperature.[1] However, until the discovery of ytterbium and calcium intercalated graphite[2,3] [$T_c(YbC_6)=6.5$ K and $T_c(CaC_6)=11.5$ K], the critical temperatures achieved were typically inferior to 5 K. Very recently, it has been shown that even higher critical temperatures (up to 15.1 K) can be achieved in CaC_6 applying hydrostatic pressure (up to 8 GPa).[4] This is presently the highest T_c reported in a GIC.

From a practical point of view GICs are appealing since carbon is a very versatile element. Beside the fact that the three most known carbon crystalline structures (fullerene, graphite, and diamond) display superconducting behavior upon intercalation[1,5] or doping,[6] carbon is also interesting for the possibility of making nanotubes which can display a superconducting behavior.[7] Moreover, the number of reagents which can be intercalated in graphite, by using chemical methods or high pressure synthesis, is very large. Consequently finding GICs with even higher critical temperatures is not a remote possibility. Therefore theoretical calculations can be a precious tool for the investigation of superconductivity in GICs.

The nature of superconductivity in intercalated GICs is still controversial. Due to their layered nature and to the presence of an intercalant band at the Fermi level (E_f), Csányi *et al.*[8] suggested a nonconventional exciton pairing mechanism.[9] On the contrary Mazin[10] proposed an electron-phonon mechanism mainly sustained by Ca vibration. In a previous work[11] we suggested that the pairing is mediated by the electron-phonon interaction. In particular the carriers are mostly electrons in the Ca Fermi surfaces coupled with Ca in-plane and C out-of-plane vibrations. The calculation of the isotope effect coefficient showed that the contribution of Ca in-plane vibrations and C out-of-plane vibrations to superconductivity is comparable.

Experimental data seem to confirm that the pairing in CaC_6 and YbC_6 is indeed due to the electron-phonon interaction, but several open questions remain. From the exponential behavior of the penetration depth in CaC_6 Lamura *et al.*[12] deduced an isotropic gap of magnitude $\Delta(0)=1.79\pm0.08$ meV. A similar isotropic gap [$\Delta(0)=1.6\pm0.2$ meV] has been measured by scanning tunneling spectroscopy.[13] The corresponding values of $2\Delta(0)/T_c$ are in agreement with the BCS theory. Similar conclusions have been obtained from the specific heat jump at the superconducting transition.[14] Thermal conductivity data in the presence of a magnetic field[15] indicate that in YbC_6 the order parameter has *s*-wave symmetry too and exclude the occurrence of multiple gaps. Isotope effect measurements[16] show a huge Ca isotope coefficient, $\alpha(Ca)=0.5$, in disagreement with theoretical calculations.[11] This is surprising, since the gap and specific heat data are correctly described by DFT calculations, meaning that the calculated electron-phonon coupling is probably correct. Even more interesting is that the total isotope effect would be probably larger than 0.5, although C-isotope effect measurements are necessary to confirm this and to judge the validity of the measurements of $\alpha(Ca)$. In any case, the large Ca-isotope coefficient, the measured superconducting gap, and the jump of the specific heat at the transition all go in favor of a phonon mediated mechanism with, most likely, a single *s*-wave gap.

In this work we want to push a step forward the prediction that can be made by the electron-phonon theory. This is important since it may allow one to identify GICs with higher critical temperatures and it also represents a significant benchmark for DFT simulations. It was noted[8] that all the superconducting GICs possess an intercalant Fermi surface at E_f. This fact is relevant for both pairing mechanisms proposed. In the case of a conventional electron-phonon mechanism the electrons in the intercalant Fermi surface are the ones strongly coupled to the phonons.[11] Thus we study the possible occurrence of superconductivity in graphite intercalated with alkaline earths (AC_6 with $A=\mathrm{Ba,Sr,Mg}$). All these GICs have an intercalant Fermi surface at E_f so they are good candidates for superconductivity. We predict the critical temperatures for BaC_6 and SrC_6 in the framework of the electron-phonon coupling theory.

As mentioned before, the critical temperature of CaC_6 and YbC_6 is enhanced with pressure. Resistivity measurements

under pressure show that, at ≈8 GPa, CaC_6 undergoes a structural phase transition to a different superconducting phase with a lower critical temperature. This structure seems to be stable at least up to 16 GPa. In other successive works magnetic[17,18] and resistive[18] measurements were performed in a much smaller range of pressures (0–1.6 GPa) and the behavior observed was confirmed. Pressure also increases the critical temperature of YbC_6 up to approximatively 7.0 K at ≈2.0 GPa. In this case too a structural transition is seen towards a different superconducting phase with lower T_c. In both YbC_6 and CaC_6 the dependence of T_c is linear with similar $\Delta T_c/\Delta P$ (0.4 for YbC_6 and 0.5 for CaC_6). The fact that T_c can be enhanced with pressure suggests that this can be a general mechanism for superconducting in GICs. It is then important to study superconductivity as a function of pressure in BaC_6, SrC_6, and finally CaC_6.

After illustrating in Secs. II and III the technical parameters and the lattice structures used in the simulations, we study the electronic structure (Sec. IV), the phonon dispersions (Sec. V), and the superconducting properties (Sec. VI) of alkaline-earth intercalated graphite at ambient pressure and at finite pressure. Particular emphasis is given to the case of CaC_6 under pressure (Sec. VII).

II. TECHNICAL DETAILS

Density functional theory (DFT) calculations are performed using the espresso code[19] and the generalized gradient approximation (GGA).[20] We use ultrasoft pseudopotentials[21] with valence configurations $3s^2 3p^6 4s^2$ for Ca, $4s^2 4p^6 4d^1 5s^1 5p^0$ for Sr, $5s^2 5p^6 5d^0 6s^2 6p^0$ for Ba, and $2s^2 2p^2$ for C. For Mg we use Troullier-Martin[22] pseudopotentials with configuration $3s^{0.1} 3p^0 3d^0$. The wave functions and the charge density are expanded using a 35 and 600 Ry cutoff. A large charge density cutoff is needed for ultrasoft potentials to obtain converged low energy phonons close to the instability for CaC_6 and SrC_6. The dynamical matrices and the electron-phonon coupling are calculated using density functional perturbation theory in the linear response.[19] For the electronic integration in the phonon calculation (structure $R\bar{3}m$) we use $N_k = 6\times6\times6$ and $N_k = 8\times8\times8$ uniform k-point meshes and Hermite-Gaussian smearing ranging from 0.1 to 0.05 Ry. In order to obtain very accurate phonon-frequencies for the low energy modes (below 15 meV) it is crucial to use a large cutoff for the charge density (600 Ry at least) and a very high convergence threshold in the phonon calculations. For the evaluation of the electron-phonon coupling and of the electronic density of states we use $N_k = 25\times25\times25$ and $N_k = 20\times20\times20$ meshes, respectively. For the λ average over the phonon momentum $\mathbf{q}$ we use a $N_q = 4\times4\times4$ $\mathbf{q}$-points mesh. The phonon dispersion is obtained by Fourier interpolation of the dynamical matrices computed on the N_q mesh.

III. CRYSTAL STRUCTURE

All the considered compounds are stage 1 (Ref. 1) at zero pressure. The atomic structure[3] of CaC_6 involves a stacked arrangement of graphene sheets (stacking AAA) with Ca atoms occupying interlayer sites above the centers of the hexagons (stacking $\alpha\beta\gamma$). The crystallographic structure is $R\bar{3}m$ where the Ca atoms occupy the $1a$ Wyckoff position (0,0,0) and the C atoms the $6g$ positions $(x,-x,1/2)$ with $x=1/6$. SrC_6 and BaC_6 have a slightly different crystal structure[23] involving a stacked arrangement of graphene sheets (stacking AAA) with Sr and Ba atoms occupying interlayer sites above the centers of the hexagons with an $\alpha\beta$ stacking. The crystallographic structure is $P6_3/mmc$ where the Sr, Ba atoms occupy the $2c$ Wyckoff position (1/3,2/3,1/4) and (1/3,2/3,3/4) and the C atoms the $12i$ positions (1/3,0,0). The experimental in-plane lattice parameter a and the interlayer spacing c for the three structures are illustrated in Table I.

TABLE I. Experimental (first two columns) structural parameters (angstrom) of BaC_6, SrC_6, CaC_6. With c we indicate the interlayer spacing, namely the distance between two graphene layers, while a is the in-plane lattice parameter. In the last two columns we report the parameters of the theoretical (LDA and GGA) $R\bar{3}m$ structure (stacking $A\alpha A\beta A\gamma$) having the same a and the same interlayer distance of the experimental structure. This rhombohedral structure is considered in all the calculations. Since MgC_6 has never been synthesized we only report its theoretical minimized structure with symmetry $R\bar{3}m$.

Material	Stacking	a,c	a,c (LDA)	a,c (GGA)
BaC_6	$A\alpha A\beta$	4.302, 5.25	4.280, 5.00	4.350, 5.20
SrC_6	$A\alpha A\beta$	4.315, 4.95	4.285, 4.80	4.325, 5.00
CaC_6	$A\alpha A\beta A\gamma$	4.333, 4.524	4.29, 4.36	4.333, 4.51
MgC_6			4.317, 3.75	4.35, 3.95

Even if the structural symmetry of SrC_6 and BaC_6 are different from the one of CaC_6, in this work we consider the same rhombohedral symmetry group (namely $R\bar{3}m$ with stacking $A\alpha A\beta A\gamma$) for all the considered GICs. We do not expect this assumption to affect qualitatively the calculated electronic and phonon properties since the two structures differ only for large distance neighbors. Indeed the distances of the first and second nearest neighbors are the same. The differences between the metal lattice sites in the $A\alpha A\beta A\gamma$ and in the $A\alpha A\beta$ structures is equivalent to those existing in the fcc and in the hcp structures.

In the last three columns of Table I we report the theoretically minimized parameters assuming the $R\bar{3}m$ structure and using the local density approximation (LDA) or the generalized gradient approximation (GGA). The interlayer distance between graphite layers (c) and the in-plane lattice parameter (a) calculated with GGA are in very good agreement with experiments. The equilibrium LDA a and c parameters are slightly compressed with respect to the CGA and experimental values.

Since MgC_6 has never been synthesized, we also assume that it crystallizes in the $R\bar{3}m$ structure. The theoretical equilibrium parameters are reported in Table I. We have verified that this structure is unstable since its energy in CGA is lower by 0.016 Ry/(cell CaC_6) than the ones of magnesium and graphite separated.

TABLE II. Theoretical (GGA) structure of alkali-earth GICs under pressure.

System	Pressure (GPa)	a	c
BaC_6	8	4.287	4.925
SrC_6	8	4.295	4.750
	16.5	4.265	4.524
CaC_6	3	4.333	4.524
	5	4.317	4.349
	6	4.314	4.330
	7	4.310	4.301
	8	4.307	4.290
	9	4.303	4.270
	10	4.300	4.250

In alkali-earth GICs as the atomic number of the intercalant (Z) is reduced the c parameter is also reduced. To disentangle the two effects we consider BaC_6, SrC_6, and CaC_6 under isotropic pressure. Since the structure of these systems at a given pressure is not known, we minimize the $R\bar{3}m$ structure at a given isotropic pressure. The lattice parameters obtained are illustrated in Table II. It should be noticed that for SrC_6 the pressure of 16.5 GPa has been chosen since the c parameter has the same value as in CaC_6 at zero pressure.

When possible, we always used the experimental a and c parameters in the electronic structure calculations. When lacking, we used the GGA minimized parameters.

IV. ELECTRONIC STRUCTURE

The zero-pressure DFT-band structures of the Ba, Sr, Ca, Mg intercalated compounds are illustrated in Fig. 1. All the considered alkali-earths intercalated GICs have at least one intercalant band at the Fermi level. This was proposed to be[8,11] a necessary condition in order to have superconductivity with a reasonable critical temperature in GICs.

The considered GICs are layered structures, but their band structures are clearly three-dimensional. This was understood in the case of CaC_6 (Ref. 11) since the rhombohedral angle (49.55°) is not too far from the one corresponding to the fcc structure (60°). The rhombohedral angles for BaC_6, SrC_6, and MgC_6 are 43.47°, 45.81°, and 55.37°, respectively. Thus the rhombohedral angle is larger as c is reduced. This is even more evident comparing the behavior of the band structure as a function of pressure in Fig. 2 for SrC_6. Note in particular that at 16.5 GPa (where the c parameter is the same as that of CaC_6 at zero pressure) the band structure is very similar to the one of CaC_6 at zero pressure. The larger bandwidths of the intercalant band as c is reduced reflects the higher three-dimensional character of the structure.

The electronic density of states for the four considered compounds are very similar (see Fig. 1) and also their values at the Fermi level are very close. No qualitative difference in the superconducting behavior of these systems can be attributed to the number of carriers at the Fermi energy [i.e., to the different value of $N(0)$].

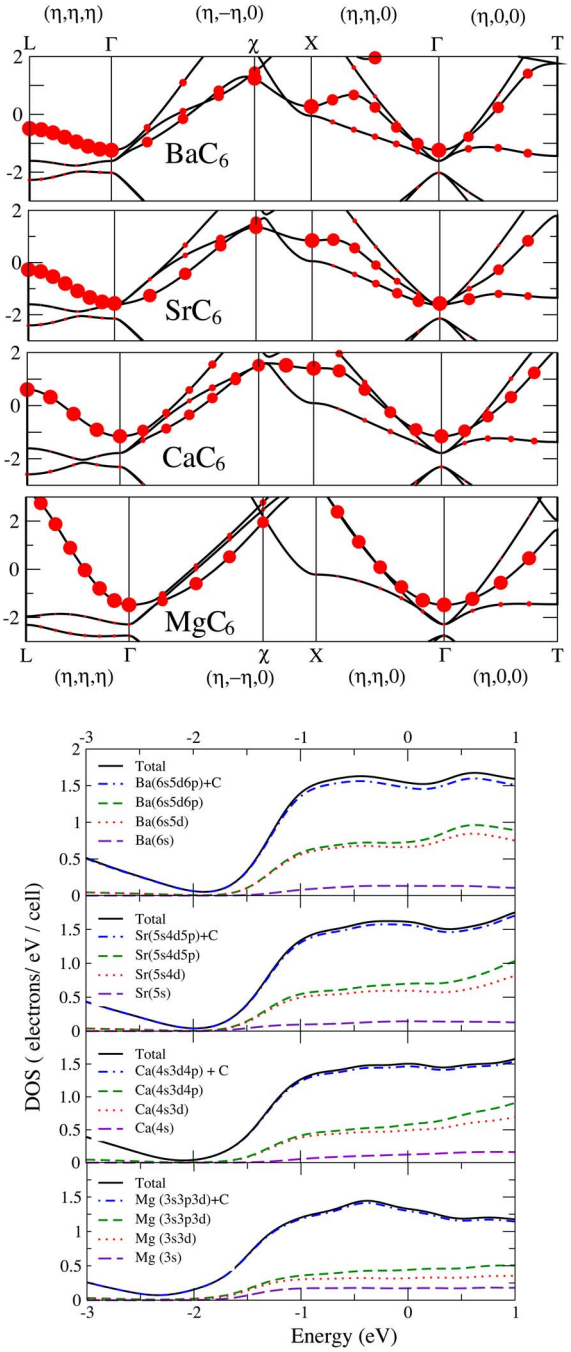

FIG. 1. (Color online) Band structure (top) and density of states projected over atomic orbitals (bottom) for several alkali-earths GICs. The zero energy corresponds to the Fermi energy. The size of the dots represents the percentage of intercalant component. As a reference, in CaC_6 the dot at ≈0.6 eV at the L point represents 95%.

The atomic-projected density of states is calculated using the Löwdin populations, $\rho_\eta(\epsilon)=\frac{1}{N_k}\Sigma_{\mathbf{k}n}|\langle\phi^L_\eta|\psi_{\mathbf{k}n}\rangle|^2\delta(\epsilon_{\mathbf{k}n}-\epsilon)$. In this expression $|\phi^L_\eta\rangle=\Sigma_{\eta'}[\mathbf{S}^{-1/2}]_{\eta,\eta'}|\phi^a_{\eta'}\rangle$ are the orthonormalized Löwdin orbitals, $|\phi^a_{\eta'}\rangle$ are the atomic wave functions, and $S_{\eta,\eta'}=\langle\phi^a_\eta|\phi^a_{\eta'}\rangle$. The density of states projected over the intercalant states has very similar value at E_f for the

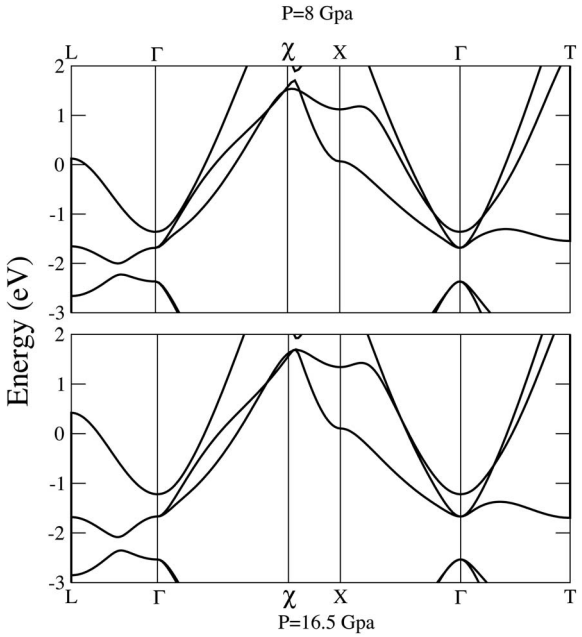

FIG. 2. Band structure of SrC_6 at different pressures. The zero of the energy corresponds to the Fermi energy.

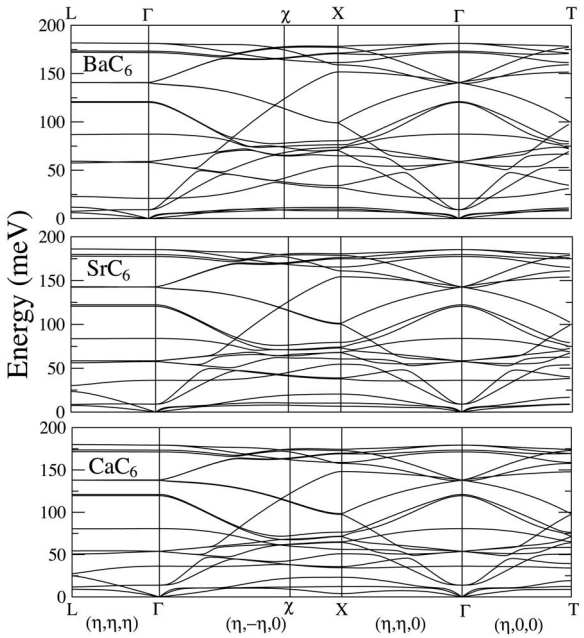

FIG. 4. Phonon dispersions of BaC_6, SrC_6, and CaC_6 at 0 GPa.

three case and it is slightly reduced with decreasing Z. No particular differences with respect to the case of CaC_6 are observed.[11] In Fig. 1 (bottom) the size of the dots represents the projection over the intercalant atomic states.

The three Fermi surface sheets of BaC_6, SrC_6, and CaC_6 are shown in Fig. 3. The sheets have been identified by the corresponding band index. As c is reduced passing from BaC_6 to CaC_6 the main difference is the change in the third sheet of the Fermi surface which is indeed a warped cylinder in BaC_6 and it becomes spherical in CaC_6. This is best seen analyzing the band structure in the ΓL direction (namely the k_z direction). In BaC_6 and SrC_6 there are no bands crossing E_f along ΓL, while in CaC_6 the Ca-originated band crosses E_f.

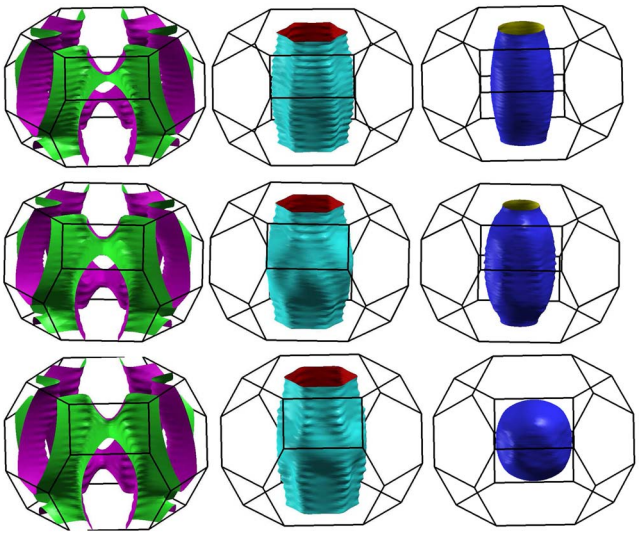

FIG. 3. (Color online) Fermi surface sheets of BaC_6, SrC_6, and CaC_6 at zero pressure. The sheets are plotted in order of increasing band index.

V. PHONON DISPERSION

The phonon dispersion of all the considered GICs can be divided into three regions. The high energy region is composed by in-plane carbon-vibration (C_{xy}), the intermediate energy region by out-of-plane carbon vibration (C_z), and the low energy region is mostly composed by intercalant vibration (I_{xy} for in-plane and I_z for out-of-plane, with I = Ba, Sr, Ca, Mg), as it was shown for CaC_6.[11] Since the high energy branches ($\omega_{\mathbf{q}\nu} > 100$ meV) are weakly affected by the type of intercalant, for the sake of clarity, in some case we only plot branches in the low energy region of the spectra. These branches are those having the greatest contribution to the electron-phonon coupling.

The zero-pressure phonon dispersion of BaC_6, SrC_6, and CaC_6 are illustrated in Figs. 4–6. As Z is reduced, and consequently c is reduced, the lowest energy branch in the ΓX direction (which corresponds to in-plane momenta with $k_z = 0$) is softened. This is evident in CaC_6 where an incipient Kohn anomaly is found at X. While the reduction of c or Z softens the I_{xy}, the intercalant I_z out-of-plane vibrations are hardened.

This effect is also apparent from the analysis of the phonon dispersion of SrC_6 and CaC_6 under pressure. In SrC_6 the lowest branch at 16 GPa in the ΓX direction is almost imaginary, meaning that at this pressure the system is close to a structural instability.[24] This instability is driven by the reduction in the c-lattice spacing. In MgC_6, at the theoretical lattice parameters (see Table I), we find imaginary phonon frequencies at X, so that the system is probably unstable. As a consequence we did not calculate the full phonon dispersion.

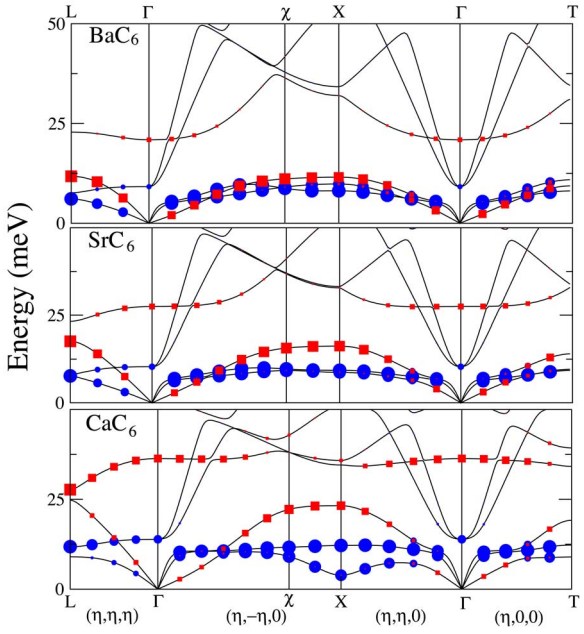

FIG. 5. (Color online) Low energy region of the phonon dispersions of BaC_6, SrC_6, and CaC_6 at 0 GPa. The size of the blue dots (red squares) represents the amount of I_{xy} (I_z), where I=Ba,Sr,Ca, vibrations.

VI. SUPERCONDUCTING PROPERTIES

The superconducting properties of alkali-earths GICs can be understood calculating the electron-phonon coupling $\lambda_{\mathbf{q}\nu}$ for a phonon mode ν with momentum $\mathbf{q}$:

$$\lambda_{\mathbf{q}\nu} = \frac{4}{\omega_{\mathbf{q}\nu} N(0) N_k} \sum_{\mathbf{k},n,m} |g^{\nu}_{\mathbf{k}n,\mathbf{k}+\mathbf{q}m}|^2 \delta(\epsilon_{\mathbf{k}n}) \delta(\epsilon_{\mathbf{k}+\mathbf{q}m}), \quad (1)$$

where the sum is over the Brillouin zone. The matrix element is $g^{\nu}_{\mathbf{k}n,\mathbf{k}+\mathbf{q}m} = \langle \mathbf{k}n | \delta V / \delta u_{\mathbf{q}\nu} | \mathbf{k}+\mathbf{q}m \rangle / \sqrt{2\omega_{\mathbf{q}\nu}}$, where $u_{\mathbf{q}\nu}$ is the amplitude of the displacement of the phonon and V is the Kohn-Sham potential. The average electron-phonon coupling is $\lambda = \Sigma_{\mathbf{q}\nu} \lambda_{\mathbf{q}\nu} / N_q$ and its value for the different compounds and for different pressures is given in Table IV.

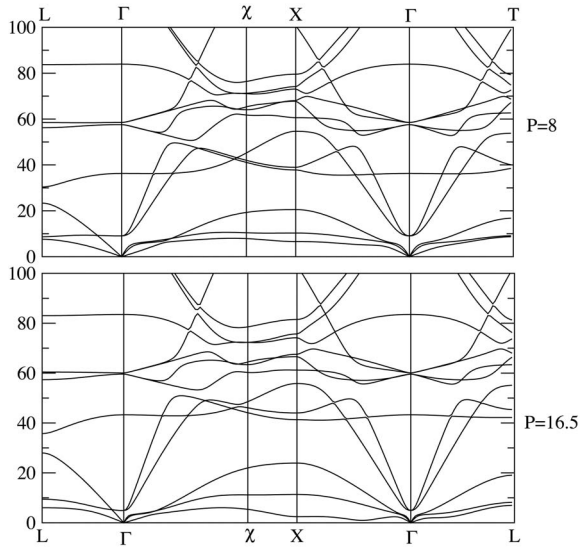

FIG. 6. Phonon dispersions of SrC_6 at 8 and 16.5 GPa.

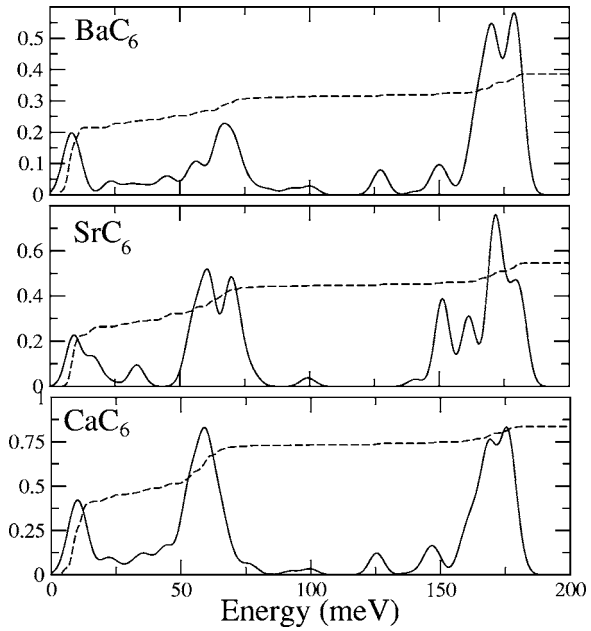

FIG. 7. Zero-pressure Eliashberg function $\alpha^2F(\omega)$ (continuous line) and integrated coupling $\lambda(\omega)$ (dashed) for BaC_6, SrC_6, and CaC_6.

The Eliashberg function

$$\alpha^2 F(\omega) = \frac{1}{2N_q} \sum_{\mathbf{q}\nu} \lambda_{\mathbf{q}\nu} \omega_{\mathbf{q}\nu} \delta(\omega - \omega_{\mathbf{q}\nu}) \quad (2)$$

and the integral $\lambda(\omega) = 2\int_{-\infty}^{\omega} d\omega' \alpha^2 F(\omega')/\omega'$ are shown in Fig. 7 for BaC_6 and SrC_6. As for CaC_6 the largest contribution to λ comes from modes below 75 meV.

An estimate of the different contributions of the in-plane and out-of-plane vibrations of the different atoms to λ can be obtained from the relation

$$\lambda = \frac{1}{N_q} \sum_{\mathbf{q}} \sum_{i\alpha j\beta} [\mathbf{G}_{\mathbf{q}}]_{i\alpha,j\beta} [\mathbf{C}_{\mathbf{q}}^{-1}]_{j\beta,i\alpha}, \quad (3)$$

where i, α indexes indicate the displacement in the Cartesian direction α of the ith atom, $[\mathbf{G}_{\mathbf{q}}]_{i\alpha,j\beta} = \Sigma_{\mathbf{k},n,m} 4 \tilde{g}^{*}_{i\alpha} \tilde{g}_{j\beta} \delta(\epsilon_{\mathbf{k}n}) \delta(\epsilon_{\mathbf{k}+\mathbf{q}m}) / [N(0) N_k]$, and $\tilde{g}_{i\alpha} = \langle \mathbf{k}n | \delta V / \delta x_{\mathbf{q}i\alpha} | \mathbf{k}+\mathbf{q}m \rangle / \sqrt{2}$. The $\mathbf{C}_{\mathbf{q}}$ matrix is the Fourier transform of the force constant matrix (the derivative of the forces respect to the atomic displacements).

Using Eq. (3) we decompose λ restricting the summation over i,α and that over i, β on two sets of atoms and Cartesian directions. The sets are C_{xy}, C_z, I_{xy}, and I_z, where I ={Ba,Sr,Ca}. The resulting $\boldsymbol{\lambda}$ matrix for the different GICs and as a function of pressure are given in Table III.

Except for SrC_6 at 16.5 GPa, the off-diagonal matrix elements are negligible. In all the cases the largest contributions to λ come from C_z and I_{xy} phonon modes. The coupling to these modes is enhanced as Z and c are reduced. A similar enhancement of C_z and I_{xy} occurs under pressure. When the

TABLE III. Decomposition of the electron-phonon coupling parameter into different vibrational components for several GICs.

	C_6Ba $P=0$			
	C_{xy}	C_z	Ba_{xy}	Ba_z
C_{xy}	0.10	0.00	−0.01	0.00
C_z	0.00	0.10	0.01	−0.01
Ba_{xy}	−0.01	0.01	0.12	−0.00
Ba_z	0.00	−0.01	0.00	0.07
	C_6Ba $P=8$			
	C_{xy}	C_z	Ba_{xy}	Ba_z
C_{xy}	0.10	0.01	−0.00	0.00
C_z	0.01	0.11	0.02	−0.01
Ba_{xy}	−0.00	0.02	0.16	−0.00
Ba_z	0.00	−0.01	−0.00	0.05
	C_6Sr $P=0$			
	C_{xy}	C_z	Sr_{xy}	Sr_z
C_{xy}	0.12	0.00	−0.00	0.00
C_z	0.00	0.20	0.02	−0.00
Sr_{xy}	−0.00	0.02	0.16	−0.00
Sr_z	0.00	−0.00	−0.00	0.05
	C_6Sr $P=8$			
	C_{xy}	C_z	Sr_{xy}	Sr_z
C_{xy}	0.12	0.01	−0.00	0.00
C_z	0.01	0.24	0.03	−0.01
Sr_{xy}	−0.00	0.03	0.19	−0.00
Sr_z	0.00	−0.01	−0.00	0.04
	C_6Sr $P=16$			
	C_{xy}	C_z	Sr_{xy}	Sr_z
C_{xy}	0.13	0.03	−0.01	0.00
C_z	0.03	0.65	0.21	−0.01
Sr_{xy}	−0.01	0.21	0.71	−0.04
Sr_z	0.00	−0.01	−0.04	0.12
	C_6Ca $P=0$			
	C_{xy}	C_z	Ca_{xy}	Ca_z
C_{xy}	0.12	0.00	−0.00	0.00
C_z	0.00	0.33	0.04	−0.01
Ca_{xy}	−0.00	0.04	0.27	−0.00
Ca_z	0.00	−0.01	−0.00	0.06
	C_6Ca $P=5$			
	C_{xy}	C_z	Ca_{xy}	Ca_z
C_{xy}	0.13	0.01	−0.00	0.00
C_z	0.01	0.35	0.03	−0.01
Ca_{xy}	−0.00	0.03	0.26	−0.01
Ca_z	0.00	−0.01	−0.01	0.05

pressure is too high, as in SrC_6 at $P=16.5$ GPa, the off-diagonal matrix elements increase and the attribution to C_z or to I_{xy} becomes ill-defined. Note also that the C_{xy} and the I_z modes are weakly affected by Z or c-axis reduction.

The critical superconducting temperature is estimated using the McMillan formula:[25]

$$T_c = \frac{\langle\omega\rangle}{1.2} e^{-1.04(1+\lambda)/[\lambda-\mu^*(1+0.62\lambda)]} \tag{4}$$

where μ^* is the screened Coulomb pseudopotential and

$$\langle\omega\rangle = e^{2/\lambda\int_0^{+\infty}\alpha^2F(\omega)\log(\omega)/\omega d\omega} \tag{5}$$

the phonon frequencies logarithmic average. Results for $\langle\omega\rangle$ and for T_c are shown in Table IV using $\mu^*=0.14$. For BaC_6 and SrC_6, T_c increases as the interlayer spacing is decreased. For SrC_6 at 16.5 GPa the result of the McMillan formula is not correct. Indeed close to the transition the increase in λ is only given by the softening of the Sr_{xy} vibration close to X. In the McMillan formula the limit $\omega_{\mathbf{q}\nu}\to 0$ implies $T_c\to 0$ as $\langle\omega\rangle$ since $\lambda_{\mathbf{q}\nu}\to\infty$ as $1/\omega^2_{\mathbf{q}\nu}$. Unfortunately the use of the McMillan formula in this limit is not correct since it deviates from the Migdal-Eliashberg (ME) results, as known from the papers of McMillan[25] and of Allen and Dynes[26] (see Fig. 1 in Ref. 26). For this reason the calculation of T_c for SrC_6 at $P=16.5$ GPa should be considered not reliable (and as a consequence it is not given in Table IV).

VII. CaC_6 UNDER PRESSURE

The study of CaC_6 under pressure needs particular emphasis due to the interest motivated by the work of Gauzzi *et al.*[4] showing a considerable increase of T_c which reaches its maximum of 15.1 K at 7 to 8 GPa. The increase of T_c has been confirmed by two other successive works measuring T_c in a much smaller range of pressure.[17,18] At 8 GPa the system seems to undergo a phase transition towards a different structure with a lower superconducting T_c.

To study the behavior of T_c under pressure we calculate the phonon dispersion and the electron-phonon coupling at 5 GPa, for which a $T_c=14$ K was detected in experiments. The comparison between the phonon dispersions at 0 and 5 GPa is shown in Fig. 8. As can be seen, while the lowest Ca phonon mode is slightly softened (mostly at X), the other Ca and C_z phonon modes are hardened. However, the overall change is fairly small and the Eliashberg functions $\alpha^2F(\omega)$ at 0 and 5 GPa have no sizable differences (see Fig. 9). At higher pressures the phonon frequencies become imaginary, similarly to what happens in SrC_6 at 16.5 GPa. In particular the largest softening occurs at X for the lowest Ca mode and it becomes negative in the range of 7–10 GPa. The lowest phonon frequency at X is extremely dependent on the Hermite-Gaussian smearing used in the calculation and as a consequence much larger k-point mesh must be used to correctly identify the phase transition (using a $10\times10\times10$ mesh and smearing 0.04 still gives results which are not converged). However, it is clear that at a sufficiently high pressure the system will become unstable and the lowest Ca phonon frequency at X will approach zero.

More insight on the superconducting properties can be gained by computing $\omega_{\log}$ and λ at 0 and 5 GPa. In this range of pressures these parameters have very similar values and consequently the critical temperature changes only slightly (see Table IV), from 11.03 K at 0 GPa to 11.40 K at 5 GPa.

The calculations for T_c under pressure are in stark disagreement with a recent theoretical calculation[17] obtained us-

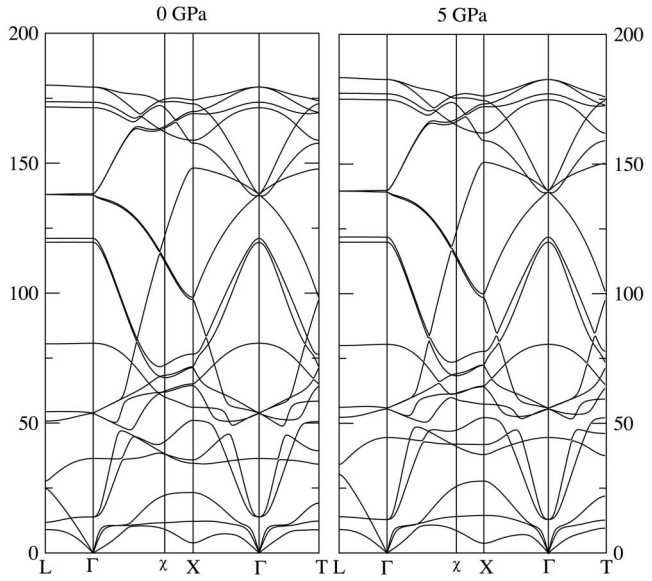

FIG. 8. Comparison between the phonon dispersion of CaC_6 at 0 and 5 GPa.

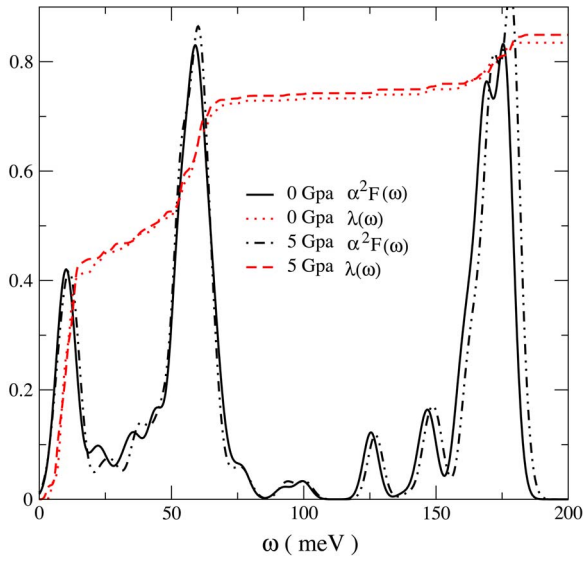

FIG. 9. (Color online) Comparison between $\alpha^2F(\omega)$ and $\lambda(\omega)$ at 0 and 5 GPa for CaC_6.

ing the same method (DFT) and the same code.

The disagreement with the calculation in Ref. 17 can be explained by the following. In Ref. 17 the electron-phonon coupling is calculated close to the structural transition (at 10 GPa) where the Ca phonon frequency strongly softens. Just before the structural transition, $\omega_{Ca} \mapsto 0$ and consequently $\lambda_{Ca} \mapsto \infty$. In this limit (close to the transition), *the behavior is highly nonlinear*. On the contrary in Ref. 17 the authors calculated T_c on the larger $4\times4\times4$ q-points mesh only at 0 and 10 GPa. The linear behavior obtained from these two points is in a slightly better agreement with experiments[27] than the actual calculation performed at several pressures. Indeed our calculation at 5.0 GPa, giving essentially the same T_c as at 0 GPa, shows that the behavior is indeed not linear and it is necessary to perform converged calculations in several points between 0 and 10 GPa.

We remark that in the calculation of the electron-phonon coupling at 0 and 5 GPa it is crucial to use at least a $4\times4\times4$ q-point mesh. If the smaller $2\times2\times2$ mesh is used, the electron-phonon coupling of the Ca modes is overestimated, since the point at X (which is included in the mesh and has a considerable electron-phonon coupling) has a too large weight. The consequent increase of T_c under pressure is much larger than in the $4\times4\times4$ mesh.

From the preceding discussion it follows that DFT calculations give a nonlinear behavior of T_c vs pressure, in stark disagreement with experiments. In particular the increase of T_c as a function of pressure is too weak when compared with experiments. In the next section we discuss what can be the origin of such a disagreement.

TABLE IV. Superconducting parameters of several GICs under pressure.

GIC	P (GPa)	λ	$\omega_{\log}$ (meV)	T_c ($\mu^*=0.14$) K
C_6Ba	0	0.38	22.44	0.23
C_6Ba	8	0.45	20.63	0.81
C_6Sr	0	0.54	28.38	3.03
C_6Sr	8	0.65	23.40	5.17
C_6Sr	16.5	1.97	3.67	nonsense
C_6Ca	0	0.83	24.70	11.03
C_6Ca	5	0.845	24.6	11.40

VIII. CONCLUSIONS

In this work we theoretically investigated the occurrence of superconductivity in graphite intercalated with alkaline earths (in particular Ba, Sr, Ca, Mg). Most of these systems have been already synthesized (BaC_6, SrC_6, and CaC_6), while MgC_6 has been proposed[10] as a good candidate for superconductivity due to its light mass and small force constants, possibly leading to large electron-phonon coupling.

We predict the critical temperatures of BaC_6 and SrC_6 to be 0.23 and 3.02 K, respectively. Moreover, we also predict a substantial increase in the critical temperature under pressure for these two systems, namely at 8 GPa the critical estimated temperatures for BaC_6 and SrC_6 are 0.81 and 5.16 K, respectively. We hope that these predictions can stimulate additional experimental work so that the nature of the pairing in GICs can be further elucidated. Moreover it would be important to judge the reliability of DFT in calculating the superconducting properties of different GICs. Indeed, while superconducting gap and specific heat measurements are in very good agreement with DFT calculations the only available measure of the Ca isotope effect[16] in CaC_6 is in stark disagreement with DFT predictions.[11] The claim that the isotope effect coefficient of Ca is 0.5, if verified by the corresponding measurement of the C isotope effect, would open different perspectives.

We have also shown that MgC_6 is energetically unstable against phase separation in Mg and graphite. Moreover, even assuming that it can be synthesized using pressure methods, the minimized structure at zero pressure obtained using DFT has imaginary phonon frequencies at the point X. Nonetheless it is interesting to note that the softening at the point X occurs when the interlayer spacing is reduced in CaC_6 and is connected to a large electron-phonon coupling at this point. This information suggests that the T_c of CaC_6 can probably be raised synthesizing $Mg_xCa_{1-x}C_y$ alloys.

Concerning CaC_6, a puzzling problem is the dependence of the critical superconducting temperature upon pressure. Experimentally T_c increases as a function of pressure, but as we have shown in this work, T_c increases much faster than what DFT calculations predict. Further work is necessary to explain the origin of this disagreement, mainly on the experimental side. Indeed diffraction data as a function of pressure are absolutely necessary. If there is a phase transformation upon pressure, the structure minimized with DFT at finite pressure would not be correct. The fact that the T_c vs pressure curves are very smooth seems to exclude an abrupt transition. A possibility is that a staging transition occurs in CaC_6 under pressure. This transition could be continuous, meaning that the staging occurs progressively in the sample. It is indeed well-known that GICs are extremely sensitive to these kinds of transitions occurring isothermally under very modest pressures. For example KC_{24}, which is a stage 2 GIC, starts a staging transition at 2.5 Kbar vs a stage 3 structure. The transition is continuous and completely achieved at $\approx$6.5 Kbar.[28] Similar transitions have been reported in Ref. 29 for MC_8 and MC_{12n} $(n=2,3,4)$ with $M=$Rb,Cs. If such a transition occurs in CaC_6 then it would not necessarily show up in the T_c vs pressures curves, but it would explain the disagreement between experiment and theory. Of course other more complicated explanations are possible, including unconventional superconductivity. In all the cases, the origin of superconductivity in intercalated GICs is not yet completely understood.

ACKNOWLEDGMENTS

We acknowledge fruitful discussions with A. Gauzzi, G. Loupias, M. d'Astuto, N. Emery, C. Herold, and L. Boeri. Calculations were performed at the IDRIS supercomputing center (Project 061202).

[1] M. S. Dresselhaus and G. Dresselhaus, Adv. Phys. **51**, 1 (2002).
[2] T. E. Weller, M. Ellerby, S. S. Saxena, R. P. Smith, and N. T. Skipper, Nat. Phys. **1**, 39 (2005); cond-mat/0503570.
[3] N. Emery, C. Hérold, M. d'Astuto, V. Garcia, Ch. Bellin, J. F. Marêché, P. Lagrange, and G. Loupias, Phys. Rev. Lett. **95**, 087003 (2005).
[4] A. Gauzzi, S. Takashima, N. Takeshita, C. Terakura, H. Takagi, N. Emery, C. Herold, P. Lagrange, and G. Loupias, cond-mat/0603443 (unpublished).
[5] O. Gunnarsson, Rev. Mod. Phys. **69**, 575 (1997).
[6] E. A. Ekimov, V. A. Sidorov, E. D. Bauer, N. N. Mel'nik, N. J. Curro, J. D. Thompson, and S. M. Stishov, Nature (London) **428**, 542 (2004).
[7] Z. K. Tang, L. Zhang, N. Wang, X. X. Zhang, G. H. Wen, G. D. Li, J. N. Wang, C. T. Chan, and P. Sheng, Science **292**, 2462 (2001).
[8] G. Csányi, P. B. Littlewood, A. H. Nevidomskyy, C. J. Pickard, and B. D. Simons, Nat. Phys. **1**, 42 (2005); cond-mat/0503569.
[9] D. Allender, J. Bray, and J. Bardeen, Phys. Rev. B **7**, 1020 (1973).
[10] I. I. Mazin, Phys. Rev. Lett. **95**, 227001 (2005).
[11] M. Calandra and F. Mauri, Phys. Rev. Lett. **95**, 237002 (2005).
[12] G. Lamura, M. Aurino, G. Cifariello, E. Di Gennaro, A. Andreone, N. Emery, C. Hérold, J. F. Marêché, and P. Lagrange, cond-mat/0601339, Phys. Rev. Lett. (to be published).
[13] N. Bergeal, V. Dubost, Y. Noat, W. Sacks, D. Roditchev, N. Emery, C. Hérold, J. F. Marêché, P. Lagrange, and G. Loupias, cond-mat/0604208 (unpublished).
[14] J. S. Kim, R. K. Kremer, L. Boeri, and F. S. Razavi, cond-mat/0603539 (unpublished).
[15] M. Sutherland, N. Doiron-Leyraud, L. Taillefer, T. Weller, M. Ellerby, and S. S. Saxena, cond-mat/0603664 (unpublished).
[16] D. G. Hinks, D. Rosenmann, H. Claus, M. S. Bailey, and J. D. Jorgensen, cond-mat/0604642 (unpublished).
[17] J. S. Kim, L. Boeri, R. K. Kremer, and F. S. Razavi, cond-mat/0603530 (unpublished).
[18] R. P. Smith, A. Kusmartseva, Y. T. C. Ko, S. S. Saxena, A. Akrap, L. Forro, M. Laad, T. E. Weller, M. Ellerby, and N. T. Skipper, cond-mat/0604204 (unpublished).
[19] http://www.pwscf.org; S. Baroni, S. de Gironcoli, A. Dal Corso, and P. Giannozzi, Rev. Mod. Phys. **73**, 515 (2001).
[20] J. P. Perdew, K. Burke, and M. Ernzerhof, Phys. Rev. Lett. **77**, 3865 (1996).
[21] D. Vanderbilt, Phys. Rev. B **41**, 7892 (1990).
[22] N. Troullier and J. L. Martins, Phys. Rev. B **43**, 1993 (1991).
[23] D. Guŕard, M. Chaabouni, P. Lagrange, M. El Makrini, and A. Hérold, Carbon **18**, 257 (1980).
[24] The results for SrC_6 at 16.5 GPa should be considered only qualitative since much larger q- and k-points mesh should be used. Moreover, very close to the structural instability anharmonic effects might become relevant.
[25] W. L. McMillan, Phys. Rev. **167**, 331 (1968).
[26] P. B. Allen and R. C. Dynes, Phys. Rev. B **12**, 905 (1975).
[27] Even assuming a linear behavior, the theoretical T_c vs pressure slope is substantially smaller than the experimental one.
[28] R. Clarke, N. Wada, and S. A. Solin, Phys. Rev. Lett. **44**, 1616 (1980).
[29] N. Wada, Phys. Rev. B **24**, 1065 (1981).